ISSN 1674-1056
http://cpb.iphy.ac.cn
http://iopscience.iop.org/cpb
中国物理 B
Chinese Physics
中国物理 Chinese Physics B

Recent progress on photoluminescence from plasmonic nanostructures: Phenomenon, mechanism, and application

Tingting Yin(尹婷婷), Liyong Jiang(蒋立勇), Zexiang Shen(申泽骧)

Citation: Chin. Phys. B . 2018, 27(9): 097803. **doi:** 10.1088/1674-1056/27/9/097803

Journal homepage: http://cpb.iphy.ac.cn; http://iopscience.iop.org/cpb

What follows is a list of articles you may be interested in

Transition intensity calculation of Yb: YAG

Hong-Bo Zhang(张洪波), Qing-Li Zhang(张庆礼), Xing Wang(王星), Gui-Hua Sun(孙贵花), Xiao-Fei Wang(王小飞), De-Ming Zhang(张德明), Dun-Lu Sun(孙敦陆)

Chin. Phys. B . 2018, 27(6): 067801. **doi:** 10.1088/1674-1056/27/6/067801

Magneto-optical properties of self-assembled InAs quantum dots for quantum information processing

Jing Tang(唐静), Xiu-Lai Xu(许秀来)

Chin. Phys. B . 2018, 27(2): 027804. **doi:** 10.1088/1674-1056/27/2/027804

Shape controllable synthesis and enhanced upconversion photoluminescence of β-$NaGdF_4$:Yb^{3+}, Er^{3+} nanocrystals by introducing Mg^{2+}

Yong-Xin Yang(杨永馨), Zheng Xu(徐征), Su-Ling Zhao(赵谡玲), Zhi-Qin Liang(梁志琴), Wei Zhu(朱薇), Jun-Jie Zhang(张俊杰)

Chin. Phys. B . 2017, 26(8): 087801. **doi:** 10.1088/1674-1056/26/8/087801

Enhancing redshift phenomenon in time-resolved photoluminescence spectra of AlGaN epilayer

Wei Li(李维), Peng Jin(金鹏), Wei-Ying Wang(王维颖), De-Feng Mao(毛德丰), Xu Pan(潘旭), Xiao-Liang Wang(王晓亮), Zhan-Guo Wang(王占国)

Chin. Phys. B . 2017, 26(7): 077802. **doi:** 10.1088/1674-1056/26/7/077802

Temperature-dependent photoluminescence of size-tunable ZnAgInSe quaternary quantum dots

Qi Ding(丁琪), Xiao-Song Zhang(张晓松), Lan Li(李岚), Jian-Ping Xu(徐建萍), Ping Zhou(周平), Xiao-Fei Dong(董晓菲), Ming Yan(晏明)

Chin. Phys. B . 2017, 26(6): 067804. **doi:** 10.1088/1674-1056/26/6/067804

TOPICAL REVIEW — Nanophotonics

Recent progress on photoluminescence from plasmonic nanostructures: Phenomenon, mechanism, and application*

Tingting Yin(尹婷婷)[2,3], Liyong Jiang(蒋立勇)[1,2,†], and Zexiang Shen(申泽骧)[2,3,‡]

[1] Department of Physics, School of Science, Nanjing University of Science and Technology, Nanjing 210094, China
[2] Center for Disruptive Photonic Technologies, School of Physical and Mathematical Sciences, Nanyang Technological University, Singapore 637371
[3] Division of Physics and Applied Physics, School of Physical and Mathematical Sciences (SPMS), Nanyang Technological University, Singapore 637371

(Received 5 March 2018; revised manuscript received 23 April 2018; published online 28 August 2018)

Photoluminescence (PL) from bulk noble metals arises from the interband transition of bound electrons. Plasmonic nanostructures can greatly enhance the quantum yield of noble metals through the localized surface plasmon. In this work, we briefly review recent progress on the phenomenon, mechanism, and application of one-photon PL from plasmonic nanostructures. Particularly, our recent efforts in the study of the PL peak position, partial depolarization, and mode selection from plasmonic nanostructures can bring about a relatively complete and deep understanding of the physical mechanism of one-photon PL from plasmonic nanostructures, paving the way for future applications in plasmonic imaging, plasmonic nanolasing, and surface enhanced fluorescence spectra.

Keywords: photoluminescence, plasmonic nanostructures, localized surface plasmon

PACS: 78.67.–n, 78.55.–m, 73.20.Mf **DOI:** 10.1088/1674-1056/27/9/097803

1. Introduction

The definition of photoluminescence (PL) is the light re-emission after absorbing a photon with energy higher than the band gap in solid physics. In semiconductors, the typical PL is from the recombination of excited electrons in the conduction band and holes in the valence band. PL from bulk noble metals and metallic nanostructures has received an enormous amount of attention in the past few decades. Initial works have revealed that when the excitation photon energy is above the direct interband transition, the one-photon PL from bulk noble metals shares the same mechanism as that of semiconductors, where a three-step process is involved: (i) photoexcitation of electron–hole pairs, (ii) relaxation of the excited electrons, and (iii) recombination of the electron–hole pairs.[1,2] Since the recombination rate of the electron–hole pairs is much slower than other nonradiative channels, the quantum efficiency of PL from bulk noble metals is extremely low (in the order of $\sim 10^{-10}$). As a comparison, PL from metallic nanostructures with a typical size larger than 50 nm is strongly modified by the localized surface plasmon resonance (LSPR), where the corresponding quantum efficiency has demonstrated to be strongly enhanced by a million times.[3–8] Pioneering study on the time-resolved PL from gold nanoparticles has also demonstrated that the LSPR can act as a radiative channel to generate ultrafast emission ($\leq$ 50 fs) comparable with the LSPR dephasing time.[9] When the excitation photon energy is below the direct interband transition, the mechanism has been contentious for the PL from bulk noble metals and metallic nanostructures. To date, main explanations include intraband excitation and emission of hot electrons,[6,10,11] as well as the prompt electronic Raman scattering.[12,13] It is hard to identify these two mechanisms from the phenomenological microcopy spectra. Despite the fact that a clear quantum mechanism still needs to be confirmed among these explanations, a universal nature of the PL normalized by the scattering spectrum has been revealed in our recent works, which emphasize an internal energy redistribution process related to the broadband PL spectrum.[14,15]

In this paper, we briefly review recent progress on the one-photon PL from plasmonic nanostructures by following the logical line of phenomenon, mechanism, and application. In Section 2, we give a simple introduction on the excitation and decay of LSPR, which plays a key role in the PL emission process from plasmonic nanostructures. In Section 3, we present our recent studies on the fundamental phenomenon and mechanism of PL from plasmonic nanostructures, including the enhancement of quantum yield through LSPR (Subsection 3.1), the comparison of peak position between PL and scattering spectra (Subsection 3.2), and the partial depolarization and mode selection during the PL emission process (Subsection 3.3). In Section 4, we briefly introduce typical engi-

*Project supported by the National Natural Science Foundation of China (Grant Nos. 61675096 and 61205042), the Natural Science Foundation of Jiangsu Province in China (Grant No. BK20141393), and the Singapore Ministry of Education Academic Research Fund Tier 3 (Grant No. MOE2011-T3-1-005) and Tier 2 (Grant No. MOE2012-T2-2-124).

†Corresponding author. E-mail: jly@njust.edu.cn
‡Corresponding author. E-mail: zexiang@ntu.edu.sg

© 2018 Chinese Physical Society and IOP Publishing Ltd

neering and application of PL from plasmonic nanostructures. In the last section, we present our conclusions and outlook.

2. Excitation and decay of localized surface plasmon

Surface plasmon is the collective oscillation of free electrons within the conduction band of the metal, which usually forms at the interface between metals and dielectrics.[3,16] Typical materials possessing the surface plasmon response include noble metals (Au, Ag, Pt) at the visible-infrared region, aluminum at the ultraviolet region, and graphene at the terahertz region. Figure 1(a) simply describes the creation of a surface plasmon oscillation and its propagating state in the waveguide, i.e., the surface plasmon polariton (SPP).[17,18] Photon-SPP coupling usually exists at the infinite metal/dielectric interface through prism or grating coupling methods. Here we focus on another type of surface plasmon which is closely related to the PL from metallic nanostructures. In the case of metallic nanostructures with sizes much less than the incident wavelength, the electron oscillations are mainly localized within the nanostructures, termed as localized surface plasmon (LSP), as shown in Fig. 1(b).[17,18] The excitation of LSPR in metallic nanoparticles results in an extreme concentration of light and an enhanced electric field around the nanostructures, leading to the significant enhancement in absorption and scattering efficiencies for photons at the resonant energy.[19] The LSPR induced strong electric field localization (hot spot) has been widely applied for surface enhanced Raman scattering (SERS), as shown in Figs. 1(c) and 1(d).[20,21]

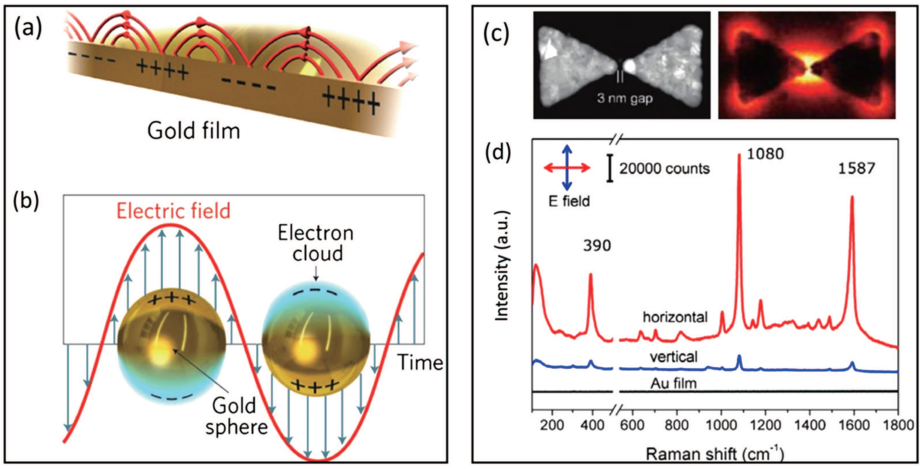


Fig. 1. (color online) Schematic of (a) surface plasmon polaritons on the surface of gold film and (b) the localized surface plasmon resonance in gold nanosphere.[22] LSPR induced hot electron generation in (c) bowtie nanostructure for (d) SERS applications.[20,21]

For simple metallic nanostructures (also called plasmonic atoms), such as nanosphere, nanorod, and nanodisk, the LSPR can act as a radiative channel to transfer the energy and momentum of LSP within metallic nanostructures to free space. Normally, the scattering light from simple metallic nanostructures exhibit different colors determined by the material they are made from, the surrounding media, the size, and shape. For example, figures 2(a) and 2(b) show the dark-field (DF) images and scattering spectra of Au nanorod, disk, and triangle, where different colors are actually determined by the different resonant energies of their LSPRs. According to the Mie scattering theory, the resonant wavelength of the fundamental LSPR is usually proportional to the nanostructure's size. As a result, the scattering color of a simple metallic nanostructure is mainly determined by its size rather than the shape.[3] However, such a conclusion is only correct for simple metallic nanostructures with sizes below the quasi-static limit. As shown in Fig. 2(c), the LSPR peak of a single Au nanodisk shows a gradual red shift with increasing size, while the LSPR response is more complicated for nanodisks with sizes beyond the quasi-static limit (a diameter larger than 140 nm). Firstly, the strength of the fundamental LSPR will gradually decrease and the high-order LSPR will be excited. Then, the resonant positions of LSPR will become more sensitive to the incident angle of the illumination light and no longer shift monotonically to the low-energy region.[23] We have successfully explained these complicated scattering spectra by accurately employing the DF illumination instead of the conventional plane wave illumination in the simulation.

For complex metallic nanostructures (also called plasmonic molecules), such as polymer, core-shell, and dolmen-like nanostructures, the inside LSPR coupling can be well described by the surface plasmon hybridization theory.[24,25] Recently, Dr. Hu measured the polarized DF scattering spectra from Au nanodisk dimers with different gaps, as shown in Fig. 2(d). The position of the excited dipolar LSPR mode under horizontal excitation consistently red shifts with decreasing gap size due to the enhanced plasmonic bonding coupling, while the mode excited under vertical excitation only blue shifts slightly due to the anti-bonding coupling.[14] Based

on the inside coupling, plasmonic color printing is one attractive application of the complex metallic nanostructures, where bright-field color prints with resolution up to the optical diffraction limitation (Figs. 2(e) and 2(f)) can be realized by tuning the diameters and separation distances of the nanodisk dimers.[26,27]

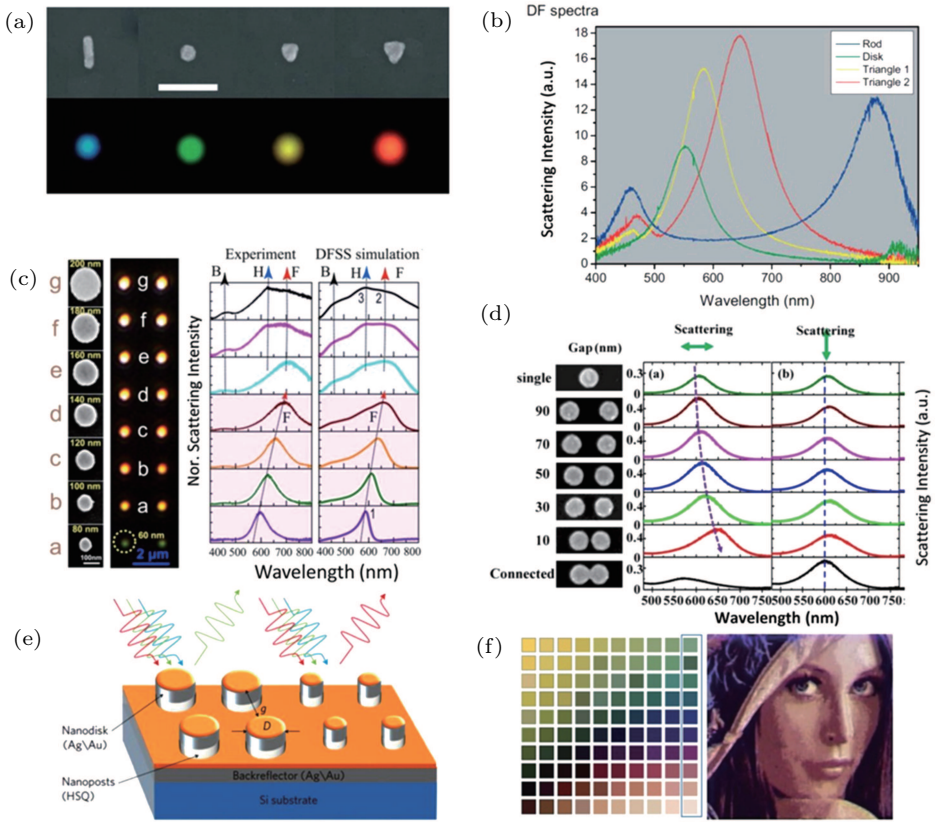


Fig. 2. (color online) (a) DF images and (b) scattering spectra of gold nanorod, disk, and two triangles.[16] (c) Scanning electron microscope (SEM), DF images, and scattering spectra of Au nanodisks with a diameter from 80 nm to 200 nm (experiment and simulation).[23] (d) SEM and DF scattering spectra of Au nanodisk dimer under horizontal and vertical excitations.[14] (e) Plasmonic subwavelength-resolution color printing realized by the interaction of nanodisks with different diameters and separations. (f) The full palette of colors and the test image.[26,27]

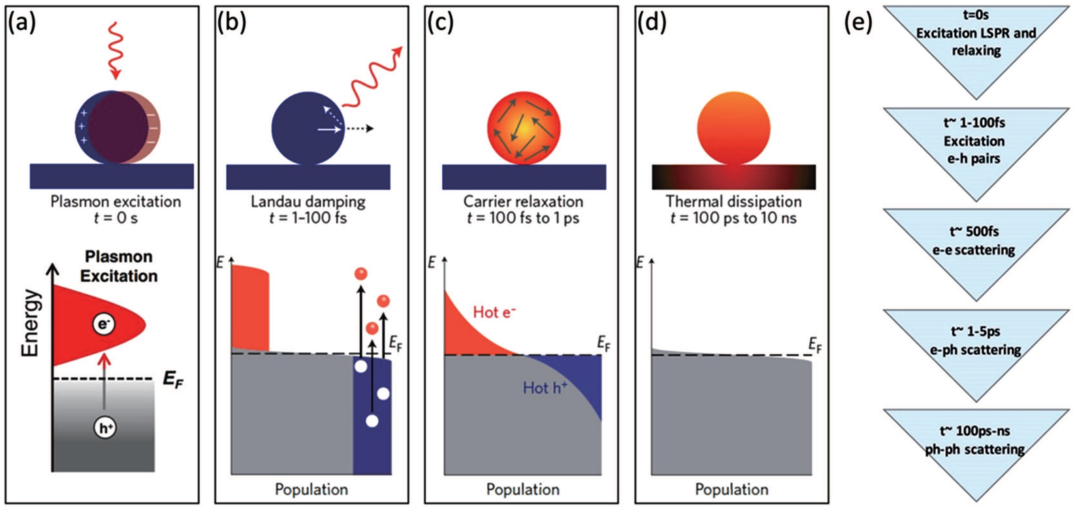


Fig. 3. (color online) Non-radiative decay process of LSPR in metal nanoparticles. Details are explained in the main text.[28]

LSPR in nanostructures can be damped radiatively by re-emission of a photon through scattering or non-radiatively through the creation and relaxation of hot electron–hole pairs (Fig. 3).[28–30] To be specific, the LSPR is excited at the initial time (Fig. 3(a)). Then the energy of LSPR can be transferred into electron–hole pairs via Landau damping on a time scale of 1–100 fs, which results in non-equilibrium hot electrons (Fig. 3(b)). Subsequently, the hot electrons generated from plasmon decay will quickly redistribute their energy among many lower-energy electrons via electron–electron scatter-

ing processes such as Auger transitions and form a quasi-equilibrium Fermi–Dirac-like distribution on a time scale of 100 fs to 1 ps (Fig. 3(c)). In the final step, the electron–phonon and phonon–phonon interactions via the lattice will dissipate the heat generated from the hot electrons into the surrounding medium on a time scale of 100 ps to 10 ns (Fig. 3(d)).

3. Photoluminescence from plasmonic nanostructures — phenomenon and mechanism

3.1. Enhanced quantum yield via LSP-mediated excitation and radiative decay

The first PL of Au film (Fig. 4(a)) with peak position $\sim$ 510 nm was observed by Mooradian in 1969,[1] which is from the radiative recombination of the sp-band electrons above the Fermi level with the d-band holes, as shown in Fig. 4(b).[6] Due to the huge nonradiative transitions, the emission quantum yield (QY) of bulk gold is extremely low in the order of $\sim 10^{-10}$.[1,4] An enhanced PL due to the strong local electric field of LSPR was first observed by Boyed *et al.* in 1986 from a rough metal surface (Fig. 4 (c)).[2,4] Then PL from metallic nanostructures aroused wide interest and significantly enhanced PL was demonstrated, where nanorod and nanotube have shown a QY in the order of $\sim 10^{-5}$ and $\sim 10^{-2}$, respectively.[4,8] Recently, Gong's group measured the QYs of PL from gold nanospheres and nanorods with different excitation wavelengths, finding that the QY is higher when the excitation energy is close to the LSPR of the nanoparticles (Figs. 4(d)–4(f)).[31] They explained that the coupling efficiency between the free electron oscillation driven by the excitation light and the intrinsic LSPR mode of the gold nanoparticles is responsible for the excitation wavelength dependent luminescence QY. To explore the gap plasmon enhancement effect, we designed a cross-like nanostructure of a Ag nanowire (NW) on a single Au nanobeam (NB) with an Al_2O_3 insulator layer (6 nm), as shown in Fig. 4(g).[32] The PL image (Fig. 4(h)) shows a hot spot at the intersection of the Ag NW and Au NB when the gap plasmon mode is excited and the absolute PL emission rate from the intersection area is higher than that from pure Au NB, as shown in Figs. 4(i) and 4(j).

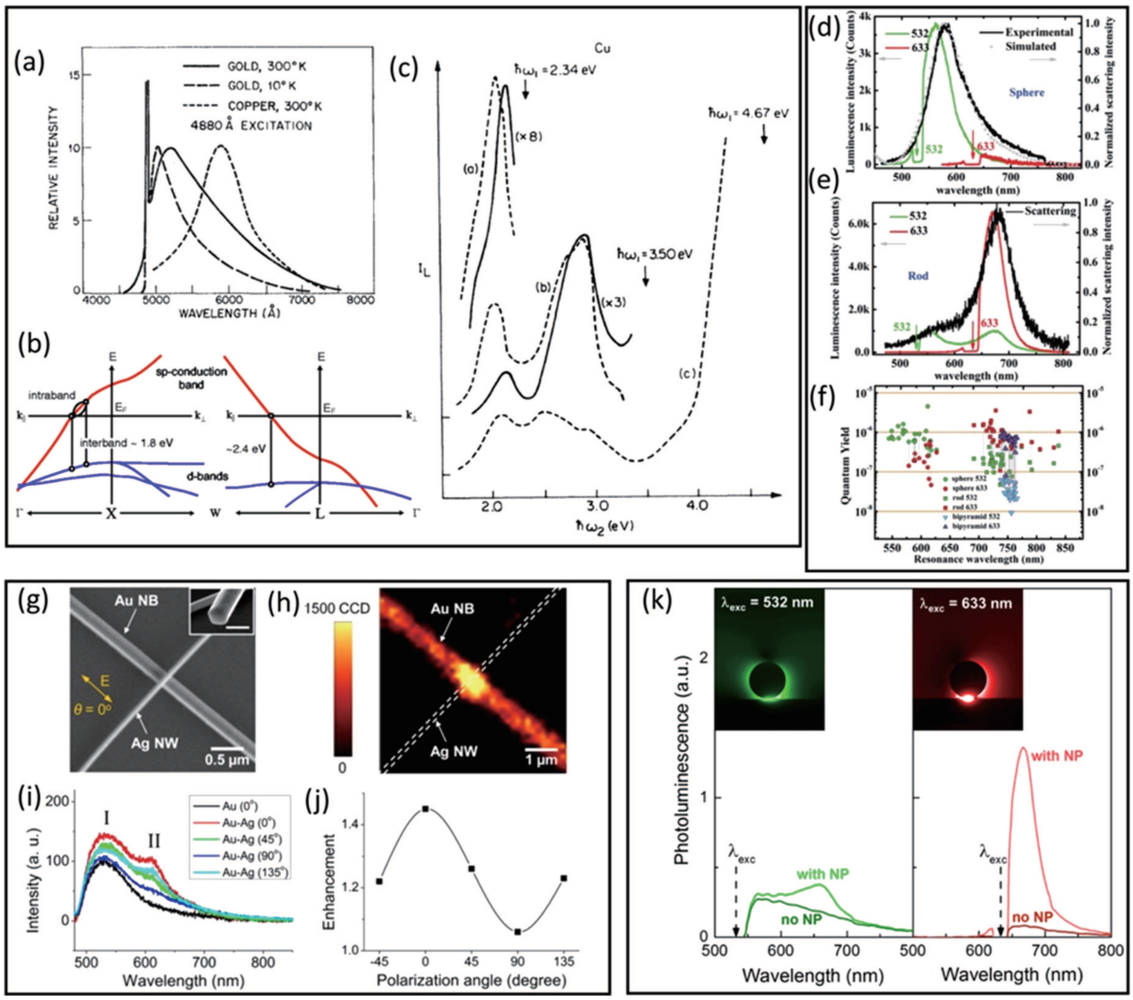


Fig. 4. (color online) (a) PL spectra of gold and copper film at room temperature.[1] (b) The band structure of gold near *X* and *L* close to the Fermi surface.[6] (c) The enhanced PL spectra from rough copper film (dashed lines) as compared to that of the smooth sample (solid lines).[2] (d)–(f) QYs of PL from gold nanoparticles are strongly dependent on the overlap between the excitation wavelengths and LSPR positions.[31] (g)–(j) Gap-plasmon enhanced PL (457 nm excitation) from a Ag nanowire on a single Au nanobeam with a 6 nm-thick Al_2O_3 insulator layer.[32] (k) Excitation wavelength dependent gap-plasmon enhanced PL from gold nanospheres on a gold film with a 3.4 nm-thick Al_2O_3 insulator layer.[33]

A similar work based on the gold nanospheres on a gold film with a 3.4 nm-thick Al_2O_3 insulator layer has demonstrated that the gap plasmon enhanced PL is also dependent on the excitation wavelength, where the magnitude of enhancement reaches up to 28000 under 633 nm excitation instead of 532 nm (far from the gap-plasmon resonance wavelength), as shown in Fig. 4(k).[33] Based on these works, the enhanced QY of PL from plasmonic nanostructures can be explained by two parts, one is from the efficient photoexcitation of bound electrons or free electron oscillation through the LSP,[2,31,33] and the other is from the efficient radiative decay from the LSPR channel.[7,34]

3.2. Peak position of PL

The peak position of PL from plasmonic nanostructures has been demonstrated to show a blue shift as compared to the corresponding scattering peak in some previous works. The first blue shift phenomenon was reported by Beversluis *et al.* in 2003,[6] where the PL peak from gold nanoparticles excited by 780 nm femtosecond pulses has shown a slight blue shift compared to the scattering peak. Such an indistinctive phenomenon was ignored for a long time. Until recently, PL studies under continuous wave (CW) laser excitation have confirmed this blue shift again in different plasmonic nanostructures.[14,35–37] Fang *et al.* in 2012 reported a slightly growing blue shift in the PL from three gold nanorods with gradually increased aspect ratio. In one of our works, Hu *et al.* in 2012 observed a more apparent size-dependent blue shift in the PL from single gold nanodisks with a diameter from 60 nm to 140 nm, where a maximum $\sim$ 50 nm blue shift was demonstrated (Fig. 5(b)).[14] Huang *et al.* in 2015 reported that this blue-shift behavior is universal for both single gold nanoparticles and gold nanodimers, as shown in Figs. 5(c) and 5(d).[36] Lin *et al.* in 2017 also observed apparent PL blue shifts from the nanorods of larger aspect ratio that resonate at longer wavelengths (Fig. 5(e)).[14] However, finding a clear physical mechanism behind the blue-shift PL behavior is still an urgent requirement. In the initial work, Beversluis *et al.* simply explained that the blue-shift PL originates from the large number of available electronic states near the interband transition edge of bulk gold.[6] In Huang *et al.*'s work, they tried to explain the blue shift by comparing the PL spectra with absorption spectra, but have not been successful yet. In our previous work,[14] we have first proposed a relatively complete explanation by assuming that PL is proportional to the production of the population profile of thermalized electrons and the density of plasmonic states (DoPS). This qualitative explanation was actually developed from Beversluis's initial explanation and it is supported by the phenomenological PL/scattering spectra of different gold nanostructures, as shown in Figs. 6(a) and 6(b). In Lin *et al.*'s work, they also agreed with our explanation and observed consistent normalized PL/scattering spectra of different nanorods (Fig. 5(e)).

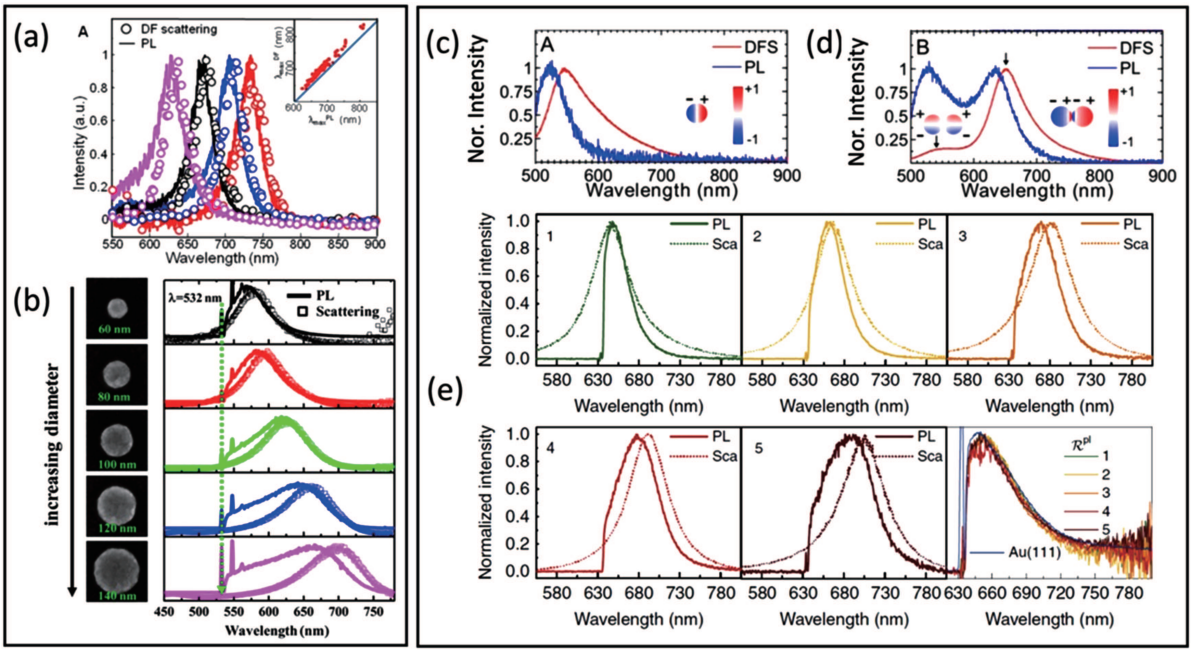


Fig. 5. (color online) (a) Comparison of PL (532 nm excitation) and DF scattering spectra of three gold nanorods with gradually increased aspect ratio.[35] (b) and (c) Comparison of PL (532 nm excitation) and DF scattering spectra of gold nanodisks with gradually increased diameter.[14] (c) and (d) Comparison of PL (488 nm excitation) and DF scattering spectra of Au monomer and dimer.[36] (e) Comparison of PL (633 nm excitation) and DF scattering spectra of five gold nanorods with gradually increased aspect ratio.[37]

Recently, we further conducted a quantitative work to support our qualitative explanation.[15] We studied the correlation of PL and DF scattering spectra of a designed dolmen-like nanostructure, which has two intrinsic LSPR modes dependent on the excitation polarization, i.e., the Lorentz-like LSPR mode under horizontal excitation and the Fano-like LSPR mode under vertical excitation. As shown in Figs. 6(c) and 6(d), the peak position of the Lorentz-like line shape PL is blue shifted ~ 20 nm relative to the DF scattering peak, while the dip position of the Fano-like line shape PL is almost stable at ~ 660 nm. The fitting results match well with the experimental spectra. As shown in Figs. 6(e) and 6(f), we have proposed a simple three-step PL process to well explain the peak and dip position behaviors.

i. **Excitation** Electrons are excited to a certain high-level state by a CW 532 nm laser (photon energy above the direct interband transition).

ii. **Relaxation** The excited electrons relax into lower-level states with population redistribution (the blue solid line).

iii. **Plasmon-modulated emission for Lorentz-like line-shape PL** The redistributed electrons radiative through the LSPR scattering channel with Lorentz-like DoPS. The observed PL is proportional to the production of the population redistribution function (PRF) of electrons and the Lorentz-like DoPS of LSPR. The PRF used in the fitting equation is an exponential decay curve extracted from the PL of bulk gold film. As a result, the PL peak position will be blue shifted via the modulation of exponential PRF.

iv. **Plasmon-modulated emission for Fano-like line-shape PL** The narrow dark mode (nonradiative) formed in the dimer interacting destructively with the bright mode in the monomer leads to an LSPR radiative channel with Fano-like DoPS. In this case, the exponential PRF can hardly affect the dip position of PL after a convolution with Fano-like DoPS.

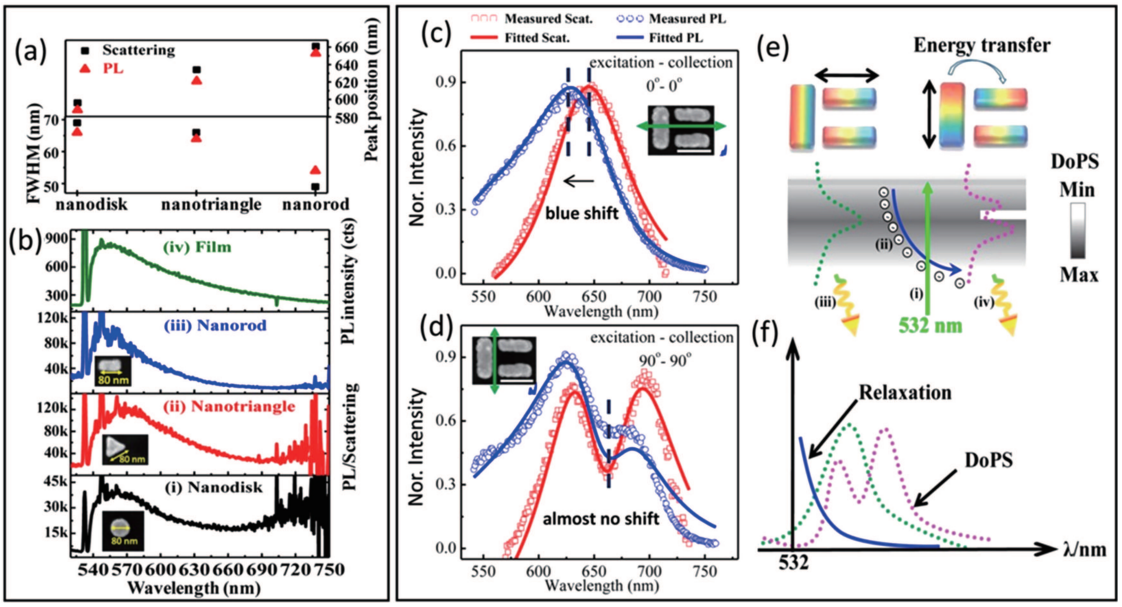


Fig. 6. (color online) (a) Comparison of PL (532 nm excitation) and DF scattering spectra of gold nanorod, gold nanotriangle, and gold nanodisk with a typical size of 80 nm.[14] (b) Comparison of the PL normalized by DF scattering spectra of three gold nanostructures and the PL from gold film. (c) and (d) Comparison of measured and fitted PL (532 nm excitation) and DF scattering spectra of dolmen-like plasmonic nanostructures. (e) A simple three-step model to describe the PL process in the dolmen-like plasmonic nanostructure. (f) Peak and dip positions of PL from the dolmen-like plasmonic nanostructure can be explained by the convolution of the PRF of electrons (solid blue curve) and the DoPS of intrinsic LSPR modes (dotted green and purple curves).[15]

We should note that a proper PRF used in our model is critical for a successful quantitative explanation on the PL peak position in arbitrary plasmonic nanostructures. The PRF is not only closely related to the nonradiative decay of bound electrons that can be modulated by the excitation energy and the crystalline quality of bulk metals, in some cases it is also closely related to the nonradiative decay of hot electrons generated by LSPR that would be strongly modulated by the size and shape of plasmonic nanostructures. An apparent blue shift of PL peak position usually occurs in the intensively decaying area of PRF,[14,15,37] while a red shift of PL peak position may occur when the scattering peak of the LSPR mode is located in the rising area of PRF.[37]

3.3. Partial depolarization and mode selection

The depolarization of PL from noble metals is a natural process due to the relaxation process of carriers,[1] during which the excited electrons go through decoherence, electron–electron and electron–phonon collisions, and they completely lost their original polarization.[38,39] As a comparison, since the scattering of LSPR is an elastic and polarization-maintaining process,[40] PL from the metallic nanostructures

through the fast-radiative decay LSPR channel[41,42] will be encoded with the same polarization characteristics of the LSPR modes.[23,43,44] When a plasmonic nanostructure is excited by a polarized laser, the excited electrons will finally radiatively decay from all intrinsic LSPR channels in the nanostructure, including the channel with the same polarization of the initial excitation laser and others with different polarizations. We called this phenomenon partial depolarization.[35,45] Figure 7(a) shows the polarization dependent PL from a single gold nanorod,[45] where both transverse and longitudinal LSPR modes can be observed no matter whether under parallel or vertical excitation-collection configurations. Figure 7(d) shows the PL from a plasmonic nanoflower, where similar partial depolarization can be observed and the depolarization ratio is found to be strongly dependent on the polarization of the excitation laser.[46] Since the plasmonic nanoflower does not have a regular shape, it is difficult to identify all possible LSPR modes in the partially depolarized PL. Figure 7(e) shows our recent work on the polarization-dependent PL from the dolmen-like plasmonic nanostructure excited under different lasers. We can confirm two intrinsic LSPR modes (Lorentz-like and Fano-like) from the PL under four excitation-collection configurations.[47] More importantly, the partially depolarized PL from such a plasmonic molecule was found to be strongly dependent on the excitation wavelength. In particular, the most apparent partial depolarization can be observed when the excitation wavelength is 532 nm that is close to the transverse LSPR of a single nanorod, indicating that the indirect energy transfer from the transverse LSPR mode to the longitudinal LSPR mode of a single nanorod plays a critical role in the partially depolarized PL from the dolmen-like plasmonic nanostructure. The indirect energy transfer between different LSPR modes can be realized via the non-radiative decay process (Fig. 3).

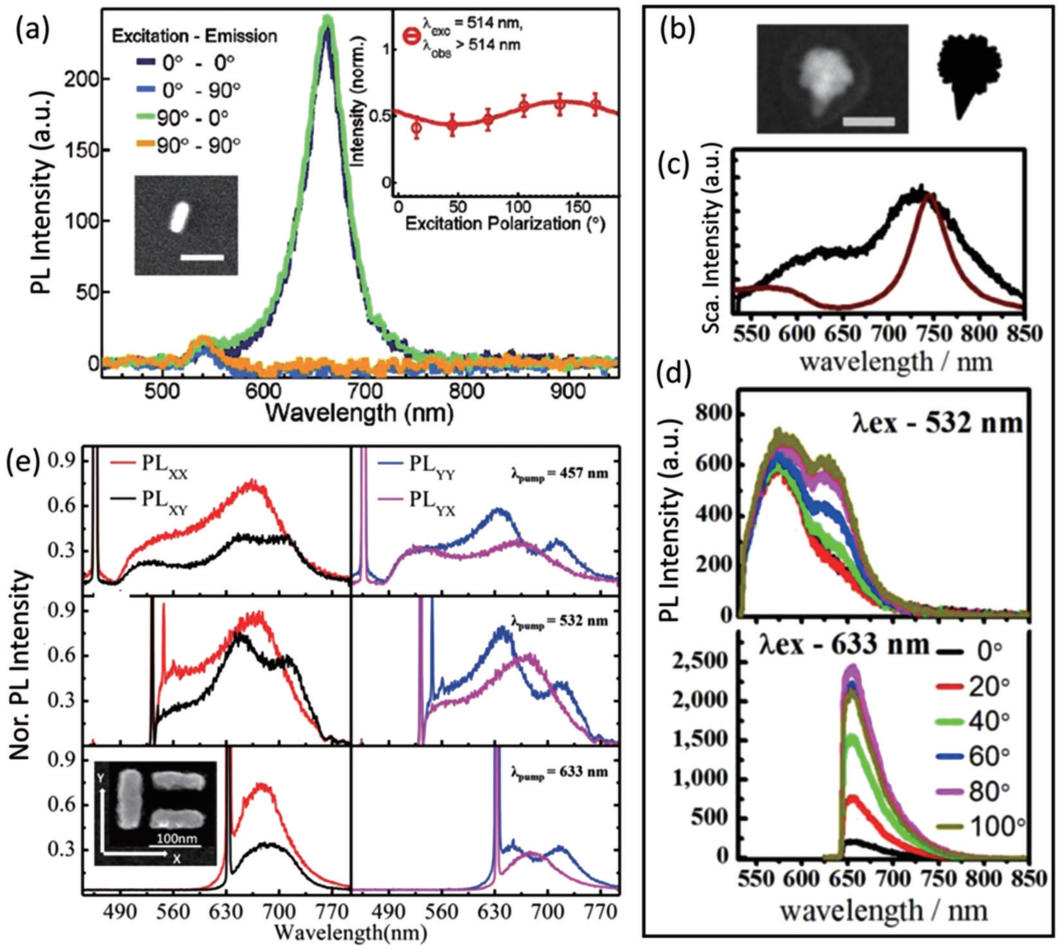


Fig. 7. (color online) (a) PL of a single gold nanorod at four orientations of excitation and detection polarizations.[45] (b) SEM image, (c) DF scattering, and (d) PL spectra of gold nanoflowers under excitation of 532 nm and 633 nm lasers with different polarization angles.[46] (e) Excitation-wavelength dependent partially depolarized PL spectra from the dolmen-like plasmonic nanostructure under four excitation-collection configurations.[47]

Mode selection in the PL from plasmonic nanostructures was reported in our recent work.[48] Figure 8(b) shows the PL from Au nanodisks with a diameter from 80 nm to 200 nm (Fig. 8(a)). It is clear to see that only fundamental LSPR mode 'a–d' can be observed for those relatively small nanodisks, while the PL spectra are dominated by the high-order LSPR mode 'g–h' for those relatively large nanodisks. The calculated absorption spectra in Fig. 8(c) clearly demonstrate that

the fundamental and high-order LSPR modes are contributed from the out-of-plan and in-plan wave vectors of the excitation laser, respectively. To further explain such mode selection phenomenon, we show the calculated absorption spectra for those relatively large nanodisks under right-side in-plan illumination in Fig. 8(d). Now both fundamental and high-order LSPR modes can be observed for those relatively large nanodisks. The preferential excitation of the high-order LSPR mode for those relatively large nanodisks in Fig. 8(b) is found due to the destructive interference under symmetric in-plan illumination. Specifically, the fundamental and high-order LSPR modes present an identical (ID) and an opposite (OP) charge distribution along the central axis of the 200 nm nanodisk (see inset), respectively. Under symmetric in-plan illumination, destructive and constructive interference will occur for the LSPR mode with ID and OP charge distribution, respectively. In our experiment, 532 nm laser was focused onto the sample with a typical size of $\sim$ 720 nm, and the incident angle was gradually increased from the spot center to the edge. As a result, those relatively large nanodisks would be more efficiently excited by the symmetric in-plan wave vectors and present a mode selection phenomenon in the PL.

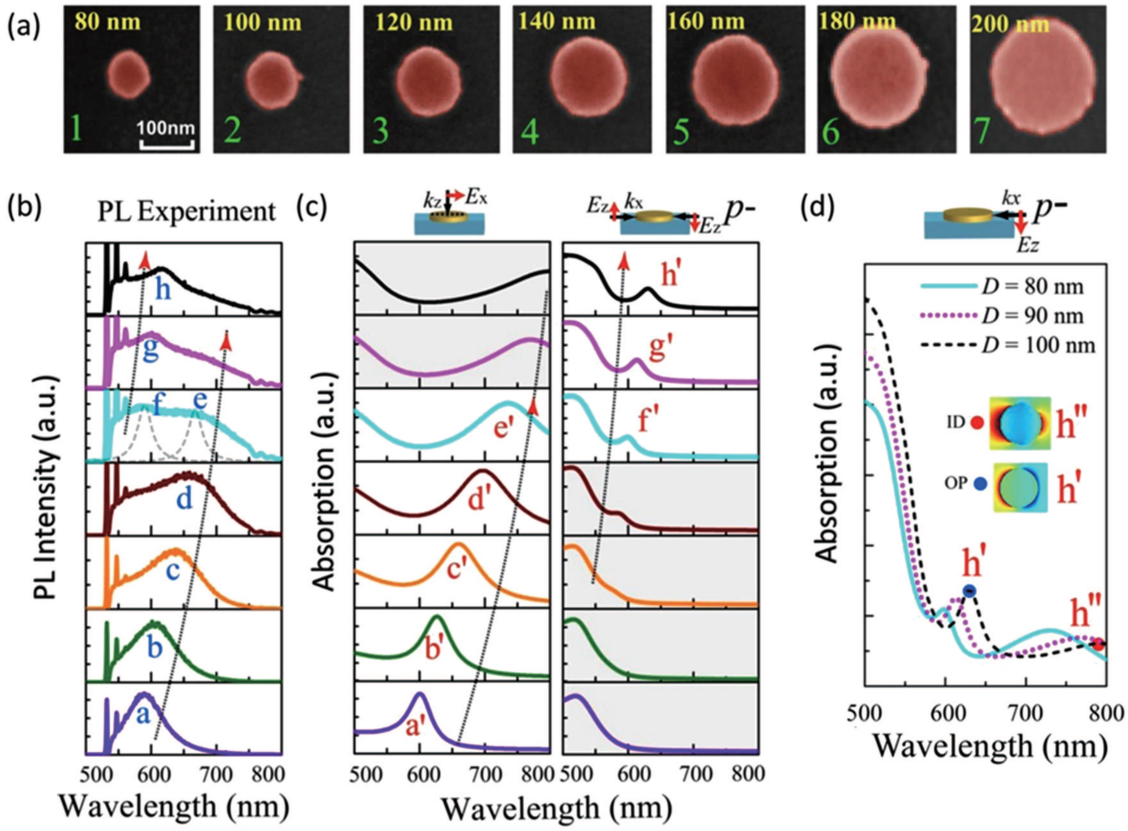


Fig. 8. (color online) (a) SEM images of Au nanodisks with a diameter from 80 nm to 200 nm. (b) Size-dependent PL from Au nanodisks under 532 nm excitation. In PL measurements, the polarization of excitation is along the horizontal direction and the collection is unpolarized. The numerical aperture of the objective lens is 0.95.[48] (c) Calculated absorption spectra of Au nanodisks under out-of-plan and symmetric in-plan illumination conditions. (d) Calculated absorption spectra of those relatively large Au nanodisks under right-side in-plan illumination. The inset shows the charge distributions of the 200 nm nanodisk for the fundamental (h″) and high-order (h′) LSPR modes.

4. Photoluminescence from plasmonic nanostructures — engineering and applications

Tailoring the linewidth of PL from plasmonic nanostructures is important for plasmonic applications which require optical resonance with high quality factors. One recent work based on the excitation of the gap plasmon mode reported significantly shrinking the linewidth of PL, where the PL linewidth of Au nanosphere dimer on metal film substrate was reduced $\sim$ 4.6 times as compared to that on the silica substrate (Fig. 9).[49] Such a narrowed PL signal presents promising applications in plasmonic nanolasing and sensing.

To date, the main applications of PL from plasmonic nanostructures have been reported in the aspects of plasmonic imaging,[8,52,53] plasmonic nanolaser,[50,54–63] and surface enhanced fluorescence (SEF).[51,64–73] Plasmonic imaging is the direct application of PL from plasmonic nanostructures and the other two belong to the indirect one. As shown in Fig. 10(a), PL from gold nanocubes with high QY of $\sim 10^{-2}$ order was successfully used in the cell imaging of human liver cancer cells (QGY) and human embryo kidney cells (293 T) with a common method of one-photon excitation.[8] The idea of plasmonic nanolaser (also called 'SPASER') was proposed in 2003 by two individual groups through different

models, i.e., gold/silica/dye core-shell nanoparticles and CdS nanorod on MaF_2/Ag film, respectively.[54–56] Extensive studies in the subsequent few years were carried out to reduce the laser threshold, improve the directional emission performance, and realize tunable wavelength of plasmonic nanolaser.[57–63] As shown in Fig. 10(b), by integrating Au nanoparticle arrays within microfluidic channels and flowing in liquid gain materials with different refractive indices, dynamic tuning of the plasmon lasing wavelength from 850 nm to 900 nm was achieved.[50] Similar to the plasmonic nanolaser, SEF of semiconductor quantum dots or dye molecules within plasmonic nanostructures has also been extensively studied in the past decade. As shown in Fig. 10(c), by suspending WSe_2 flakes onto sub-20-nm-wide trenches in a gold substrate, a giant PL enhancement of $\sim$ 20000 fold was demonstrated due to the lateral gap plasmons confined in the trenches and the enhanced Purcell factor by the plasmonic nanostructure.[51] Besides these typical applications, Ren's group recently proposed a method to retrieve the fingerprint of intrinsic chemical information from the SERS spectra based on the PL from the plasmonic nanostructures in SERS (Fig. 11(d)).[37] The method is established based on the explanation that the SERS background originates from the LSPR-modulated PL, which contains the local field information shared by SERS.[12]

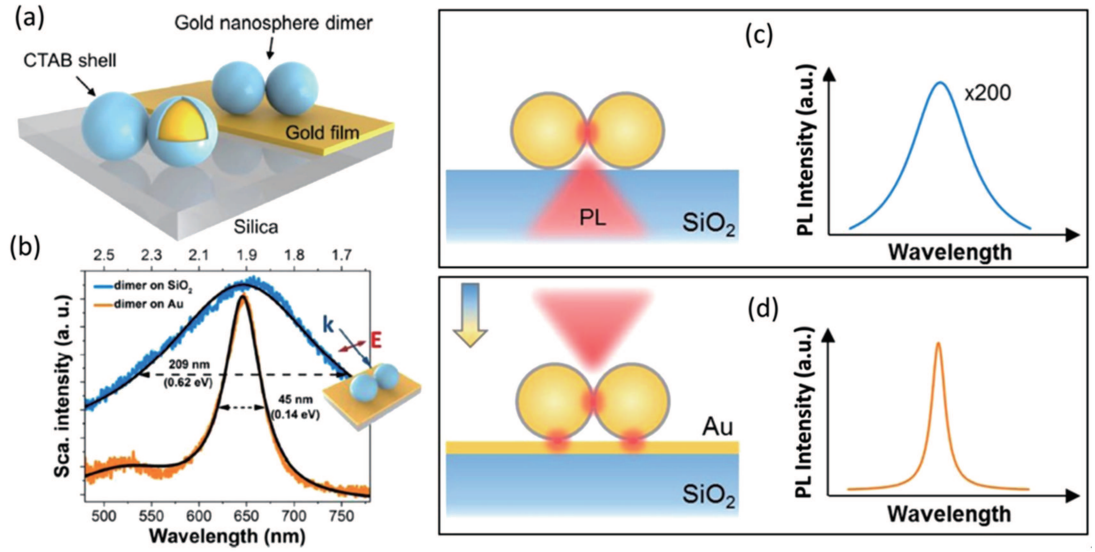


Fig. 9. (color online) (a) Schematic of two CTAB-coated (light blue) Au nanosphere dimers positioned on a thin Au film (yellow) and on the silica substrate (light gray) respectively. (b) Measured scattering spectra and PL spectra of the Au nanosphere dimmers (c) on the Au film and (d) on the silica substrate.[49]

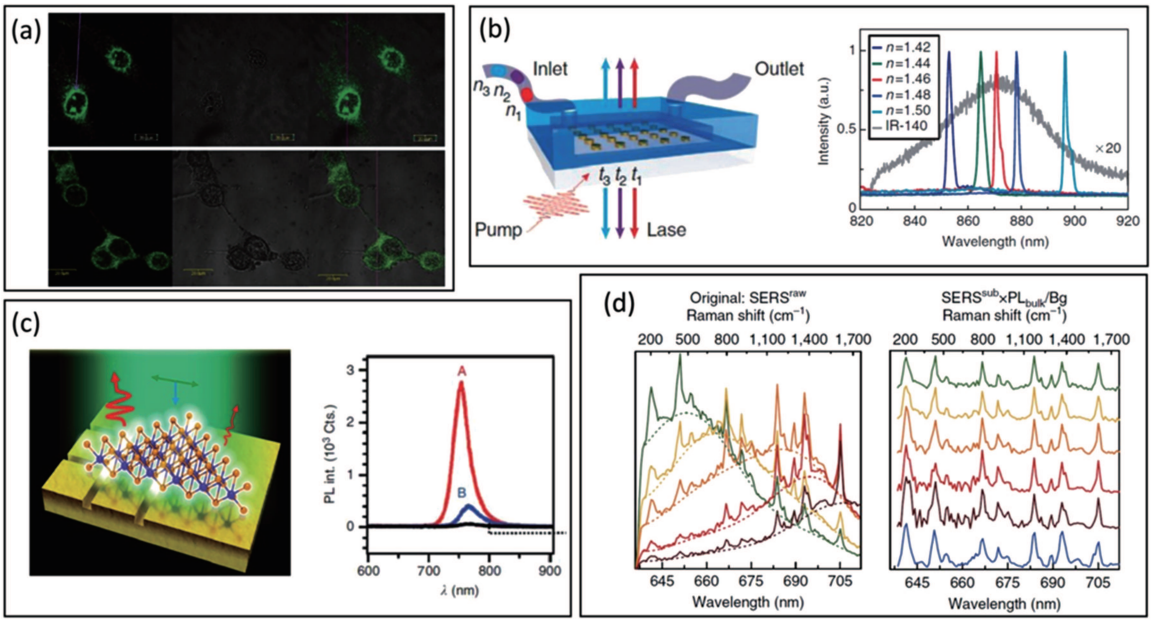


Fig. 10. (color online) (a) Plasmonic PL with high QY can be used for cell imaging applications.[8] (b) Real-time tunable lasing from plasmonic nanocavity arrays.[50] (c) Giant PL enhancement in tungsten-diselenide-gold plasmonic hybrid structures.[51] (d) Plasmonic PL for recovering native chemical information from SERS.[37]

5. Conclusions and outlook

Based on the pioneering works and our recent new findings, we summarize here a relatively complete mechanism of one-photon PL from plasmonic nanostructures in the following three steps. (i) Excitation. Bound electrons or free electron oscillation can be excited to a certain state through interband transition or intraband transition, respectively. The excitation can be greatly enhanced when the energy of the excitation laser is overlapped with the LSPR mode. (ii) Relaxation. Excited electrons relax into the continuous lower-energy states with population redistribution. (iii) LSPR-modulated emission. LSPR acts as an ultrafast radiative decay channel for the excited electrons and can greatly enhance the QY of emission. PL from plasmonic nanostructures is proportional to the production of the PRF of electrons and the DoPS of LSPR modes, during which the peak position of PL can be modulated by the specific PRF in plasmonic nanostructures. Enhanced partially depolarized PL can be generated due to the indirect energy transfer between intrinsic LSPR modes via excitation and relaxation of hot electrons. Mode selection phenomenon can occur in the PL from plasmonic nanostructures due to the preferential excitation of LSPR mode under symmetric in-plan illumination. The fundamental phenomenon and mechanism of anti-Stokes one-photon emission,[74] two-photon and multiphoton emission,[75–78] and nonlinear phenomenon[79–81] in the PL from plasmonic nanostructures will be reviewed in our future work.

The application of PL from plasmonic nanostructures is currently focused on the plasmonic nanolaser and SEF. Many urgent scientific issues such as the laser threshold, the reproducibility of plasmonic nanolasers,[82] and the interaction between fluorescence molecules and plasmonic nanostructures require deeper studies.[83] Metamaterials and plasmonic-optical hybrid platforms are expected to attract more attention for plasmonic nanolasers and SEF applications.[84,85]

References

[1] Mooradian A 1969 *Phys. Rev. Lett.* **22** 185
[2] Boyd G T, Yu Z H and Shen Y R 1986 *Phys. Rev. B* **33** 7923
[3] Link S and El-Sayed M A 2000 *Int. Rev. Phys. Chem.* **19** 409
[4] Mohamed M B, Volkov V, Link S and El-Sayed M A 2000 *Chem. Phys. Lett.* **317** 517
[5] Huang T and Murray R W 2003 *J. Phys. Chem. B* **107** 7434
[6] Beversluis M R, Bouhelier A and Novotny L 2003 *Phys. Rev. B* **68** 115433
[7] Dulkeith E, Niedereichholz T, Klar T A, Feldmann J, Von Plessen G, Gittins D I, Mayya K S and Caruso F 2004 *Phys. Rev. B* **70** 205424
[8] Wu X, Ming T, Wang X, Wang P N, Wang J F and Chen J Y 2010 *ACS Nano* **4** 113
[9] Varnavski O P, Goodson T, Mohamed M B and El-Sayed M A 2005 *Phys. Rev. B* **72** 235405
[10] Haug T, Klemm P, Bange S and Lupton J M 2015 *Phys. Rev. Lett.* **115** 067403
[11] Lin K Q, Yi J, Hu S, Sun J J, Zheng J T, Wang X and Ren B 2016 *ACS Photon.* **3** 1248
[12] Hugall J T and Baumberg J J 2015 *Nano Lett.* **15** 2600
[13] Mertens J, Kleemann M E , Chikkaraddy R, Narang P and Baumberg J J 2017 *Nano Lett.* **17** 2568
[14] Hu H L, Duan H G, Yang J K W and Shen Z X 2012 *ACS Nano* **6** 10147
[15] Yin T T, Dong Z G, Jiang L Y, Zhang L, Hu H, Qiu C W, Yang J K W and Shen Z X 2016 *ACS Photon.* **3** 979
[16] Murray W A and Barnes W L 2007 *Adv. Mater.* **19** 3771
[17] Amendola V, Pilot R, Frasconi M, Marago O M and Iati M A 2017 *J. Phys.: Condens. Matter* **29** 203002
[18] Maier S A 2007 *Plasmonics: Fundamentals and Applications* (New York: Springer) p. XXVI
[19] Wang F and Shen Y R 2006 *Phys. Rev. Lett.* **97** 206806
[20] Duan H G, Hu H L, Hui H K, Shen Z X and Yang J K W 2013 *Nanotechonology* **24** 185301
[21] Duan H G, Fernández-Domínguez A I, Bosman M, Maier S A and Yang J K W 2012 *Nano Lett.* **12** 1683
[22] Liang Z Q, Sun J, Jiang Y Y, Jiang L and Chen X D 2014 *Plasmonics* **9** 859
[23] Jiang L Y, Yin T T, Dong Z G, Liao M Y, Tan S J, Goh X M, Allioux D, Hu H L, Li X Y, Yang J K W and Shen Z 2015 *ACS Nano* **9** 10039
[24] Jain P K and El-Sayed M A 2010 *Chem. Phys. Lett.* **487** 153
[25] Prodan E, Radloff C, Halas N J and Nordlander P 2003 *Science* **302** 419
[26] Kumar K, Duan H G, Hegde R S, Koh S C W, Wei J N and Yang J K W 2012 *Nat. Nanotechnol.* **7** 557
[27] Kristensen A, Yang J K W, Bozhevolnyi S I, Link S, Nordlander P, Halas N J and Mortensen N A 2017 *Nat. Rev. Mater.* **2** 16088
[28] Brongersma M L, Halas N J and Nordlander P 2015 *Nat. Nanotechnol.* **10** 25
[29] Klar T, Perner M, Grosse S, Von Plessen G, Spirkl W and Feldmann J 1998 *Phys. Rev. Lett.* **80** 4249
[30] Watanabe K, Menzel D, Nilius N and Freund H J 2006 *Chem. Rev.* **106** 4301
[31] Cheng Y Q, Lu G W, He Y B, Shen H M, Zhao J Y, Xia K Y and Gong Q H 2016 *Nanoscale* **8** 2188
[32] Wan A, Wang T, Yin T T, Lo A R, Hu H L, Li S Z, Shen Z X and Nijhuis C A 2015 *ACS Photon.* **2** 1348
[33] Lumdee C, Yun B F and Kik P G 2014 *ACS Photon.* **1** 1224
[34] Shahbazyan T V 2013 *Nano Lett.* **13** 194
[35] Fang Y, Chang W S, Willingham B, Swanglap P, Dominguez-Medina S and Link S 2012 *ACS Nano* **6** 7177
[36] Huang D, Byers C P, Wang L Y, Hoggard A L, Hoenee B, Dominguez-Medina S, Chen S S, Chang W S, Landes C F and Link S 2015 *ACS Nano* **9** 7072
[37] Lin K Q, Yi J, Zhong J H, Hu S, Liu B J, Liu J Y, Zong C, Lei Z C, Wang X, Aizpurua J, Esteban R and Ren B 2017 *Nat. Commun.* **8** 14891
[38] Voisin C, Christofilos D, Loukakos P A, Del F N, Vallee F, Lerme J, Gaudry M, Cottancin E, Pellarin M and Broyer M 2004 *Phys. Rev. B* **69** 195416
[39] Bauer M, Marienfeld A and Aeschlimann M 2015 *Progr. Surf. Sci.* **90** 319
[40] Lassiter J B, Aizpurua J, Hernandez L I, Brandl D W, Romero I, Lal S, Hafner J H, Nordlander P and Halas N J 2008 *Nano Lett.* **8** 1212
[41] Bouhelier A, Bachelot R, Lerondel G, Kostcheev S, Royer P and Wiederrecht G P 2005 *Phys. Rev. Lett.* **95** 267405
[42] Knittel V, Fischer M P, De Roo T, Mecking S, Leitenstorfer A and Brida D 2015 *ACS Nano* **9** 894
[43] Chen W L, Lin F C, Lee Y Y, Li F C, Chang Y M and Huang J S 2014 *ACS Nano* **8** 9053
[44] Andersen S K H, Pors A and Bozhevolnyi S I 2015 *ACS Photon.* **2** 432
[45] Tcherniak A, Dominguez-Medina S, Chang W S, Swanglap P, Slaughter L S, Landes C F and Link S 2011 *J. Phys. Chem. C* **115** 15938
[46] Zhang T Y, Lu G W, Shen H M, Shi K B, Jiang Y Y, Xu D S and Gong Q H 2015 *Sci. Rep.* **4** 3867
[47] Yin T T, Jiang L Y, Dong Z G, Yang J K W and Shen Z X 2017 *Nanoscale* **9** 2082
[48] Jiang L Y, Yin T T, Dong Z G, Hu H L, Liao M Y, Allioux D, Tan S J, Goh X M, Li X Y, Yang J K W and Shen Z X 2015 *ACS Photon.* **2** 1217
[49] Li G C, Zhang Y L, Jiang J, Luo Y and Lei D Y 2017 *ACS Nano* **11** 3067
[50] Yang A K, Hoang T B, Dridi M, Deeb C, Mikkelsen M H, Schatz G C and Odom T W 2015 *Nat. Commun.* **6** 6939

[51] Wang Z, Dong Z G, Gu Y H, Chang Y H, Zhang L, Li L J, Zhao W J, Eda G, Zhang W J, Grinblat G, Maier S A, Yang J K W, Qiu C W and Wee A T S 2016 *Nat. Commun.* **7** 11283

[52] Shang L, Dorlich R M, Brandholt S, Schneider R, Trouillet V, Bruns M, Gerthsen D and Nienhaus G U 2011 *Nanoscale* **3** 2009

[53] Yang X, Yang M X, Pang B, Vara M and Xia Y N 2015 *Chem. Rev.* **115** 10410

[54] Bergman D J and Stockman M I 2003 *Phys. Rev. Lett.* **90** 027402

[55] Noginov M A, Zhu G, Belgrave A M, Bakker R, Shalaev V M, Narimanov E E, Stout S, Herz E, Suteewong T and Wiesner U 2009 *Nature* **460** 1110

[56] Oulton R F, Sorger V J, Zentgraf T, Ma R M, Gladden C, Dai L, Bartal G and Zhang X 2009 *Nature* **461** 629

[57] Flynn R A, Kim C S, Vurgaftman I, Kim M, Meyer J R, Mäkinen A J, Bussmann K, Cheng L, Choa F S and Long J P 2011 *Opt. Express* **19** 8954

[58] Meng X G, Kildishev A V, Fujita K, Tanaka K and Shalaev V M 2013 *Nano Lett.* **13** 4106

[59] Shi C, Soltani S and Armani A M 2013 *Nano Lett.* **13** 5827

[60] Khurgin J B and Sun G 2014 *Nat. Photon.* **8** 468

[61] Lu Y J, Wang C Y, Kim J S, Chen H Y, Lu M Y, Chen Y C, Chang W H, Chen L J, Stockman M I, Shih C K and Gwo S 2014 *Nano Lett.* **14** 4381

[62] Yang A K, Li Z Y, Knudson M P, Hryn A J, Wang W J, Aydin K and Odom T W 2015 *ACS Nano* **9** 11582

[63] Galanzha E I, Weingold R, Nedosekin D A, Sarimollaoglu M, Nolan J, Harrington W, Kuchyanov A S, Parkhomenko R G, Watanabe F, Nima Z, Biris A S, Plekhanov A I, Stockman M I and Zharov V P 2017 *Nat. Commun.* **8** 15528

[64] Tanaka K, Plum E, Ou J Y, Uchino T and Zheludev N I 2010 *Phys. Rev. Lett.* **105** 227403

[65] Ayala-Orozco C, Liu J G, Knight M W, Wang Y, Day J K, Nordlander P and Halas N J 2014 *Nano Lett.* **14** 2926

[66] Najmaei S, Mlayah A, Arbouet A, Girard C, Léotin J and Lou J 2014 *ACS Nano* **8** 12682

[67] Yu S J, Kim Y H, Lee S Y, Song H D and Yi J 2014 *Angew. Chem. Int. Ed.* **53** 11203

[68] Zheng Z K, Tachikawa T and Majima T 2015 *J. Am. Chem. Soc.* **137** 948

[69] Chen H T, Yang J, Rusak E, Straubel J, Guo R, Myint Y W, Pei J J, Decker M, Staude I, Rockstuhl C, Lu Y R, Kivshar Y S and Neshev D 2016 *Sci. Rep.* **6** 22296

[70] Lee G Y, Jung K, Jang H S, Kyhm J, Han I K, Park B, Ju H, Kwon S J and Ko H 2016 *Nanoscale* **8** 2071

[71] Johnson A D, Cheng F, Tsai Y and Shih C K 2017 *Nano Lett.* **17** 4317

[72] Yan J H, Ma C R, Liu P and Yang G W 2017 *ACS Photon.* **4** 1092

[73] Signoretto M, Zink-Lorre N, Martínez-Pastor J P, Font-Sanchis E, Chirvony V S, Sastre-Santos Á, Fernández-Lázaro F and Suárez I 2017 *Appl. Phys. Lett.* **111** 081102

[74] He Y B, Xia K Y, Lu G W, Shen H M, Cheng Y Q, Liu Y C, Shi K B, Xiao Y F and Gong Q H 2015 *Nanoscale* **7** 577

[75] Guan Z P, Gao N Y, Jiang X F, Yuan P Y, Han F and Xu Q H 2013 *J. Am. Chem. Soc.* **135** 7272

[76] Verellen N, Denkova D, Clercq B D, Silhanek A V, Ameloot M, Dorpe P V and Moshchalkov V V 2015 *ACS Photon.* **2** 410

[77] Molinaro C, El Harfouch Y, Palleau E, Eloi F, Marguet S, Douillard L, Charra F and Fiorini-Debuisschert C 2016 *J. Phys. Chem. C* **120** 23136

[78] Masuo S, Kanetaka K, Sato R and Teranishi T 2016 *ACS Photon.* **3** 109

[79] Knittel V, Fischer M P, Vennekel M, Rybka T, Leitenstorfer A and Brida D 2017 *Phys. Rev. B* **96** 125428

[80] Lien M B, Kim J Y, Han M G, Chang Y C, Chang Y C, Ferguson H J, Zhu Y, Herzing A A, Schotl, J C, Kotov N A and Norris T B 2017 *ACS Nano* **11** 5925

[81] Huang J, Wang W, Murphy C J and Cahill D G 2014 *Proc. Natl Acad. Sci. USA* **111** 906

[82] Shangjr G and Chih-Kang S 2016 *Rep. Prog. Phys.* **79** 086501

[83] Dong J, Zhang Z L, Zheng H R and Sun M T 2017 *Nanophotonics* **6** 502

[84] Wang X L, Morea R, Gonzalo J and Palpant B 2015 *Nano Lett.* **15** 2633

[85] Cui S Y, Zhang X Y, Liu T L, Lee J, Bracher D, Ohno K, Awschalom D and Hu E L 2015 *ACS Photon.* **2** 465